

Polarization and relaxation rates of radon

E. R. Tardiff,¹ J. A. Behr,³ T. E. Chupp,¹ K. Gulyuz,⁴ R. S. Lefferts,⁴ W. Lorenzon,² S. R. Nuss-Warren,¹ M. R. Pearson,³ N. Pietralla,⁴ G. Rainovski,⁴ J. F. Sell,⁴ and G. D. Sprouse⁴

¹*FOCUS Center, University of Michigan Physics Department, 450 Church Street, Ann Arbor, Michigan 48109-1040, USA*

²*University of Michigan Physics Department, 450 Church Street, Ann Arbor, Michigan 48109-1040, USA*

³*TRIUMF, 4004 Westbrook Mall, Vancouver V6T 2A3, Canada*

⁴*SUNY Stony Brook Department of Physics and Astronomy, Stony Brook, New York 11794-3800, USA*

(Received 10 January 2008; published 23 May 2008)

Polarization and relaxation of radon isotopes by spin exchange with laser optically pumped rubidium were studied in preparation for electric dipole moment measurements with octupole deformed ^{223}Rn . γ -ray anisotropies provided a measure of nuclear polarization produced by spin exchange with laser polarized rubidium vapor, and the temperature dependence over the range 130 to 220°C was measured to parametrize the spin exchange polarization and the quadrupole-dominated wall relaxation rate. These results provide quantitative data for developing electric dipole moment measurements of octupole-deformed ^{223}Rn and other radon isotopes.

DOI: 10.1103/PhysRevC.77.052501

PACS number(s): 32.10.Dk, 11.30.-j, 23.20.En, 23.20.Gq

Polarization of noble gas atoms by spin exchange with laser optically pumped alkali-metal atoms has provided samples of gas for a wide variety of investigations. Laser polarized ^3He finds wide application in lung imaging [1], in studies of nucleon structure by polarized electron scattering [2], and in studies with polarized neutrons [3]. Laser polarized ^{129}Xe has been used in extensive studies of the spin-exchange process [4] and in biomedical imaging and blood flow measurement [5]. Other species such as ^{21}Ne and radon isotopes have applications in fundamental measurements including tests of Lorentz invariance [6,7] and the search for a Charge-conjugation and Parity Symmetry (CP) violating permanent electric dipole moment (EDM). An EDM is a separation of charge along the angular momentum of a system that violates Time-Reversal Symmetry (T) and parity (P) invariance because it is a T-even polar vector and the spin is a T-odd axial vector. Assuming Charge-conjugation, Parity and Time-reversal Symmetry (CPT), T violation implies CP violation; thus an atomic system would acquire an EDM due to interactions of the atomic electrons with a CP-violating distribution of charge in the nucleus, due to the intrinsic EDM of an unpaired electron, or due to a CP-violating component of the electron-nuclear force. Measurement of a finite EDM would probe physics beyond the standard model such as that necessary to explain the cosmological baryon asymmetry in the context of Sakharov's model of baryogenesis [8].

The EDM of ^{223}Rn is of particular interest due to the potential for the large enhancement of the CP-violating nuclear Schiff moment in the octupole deformed nucleus [9–11]. Generic CP-violating mechanisms would produce an atomic EDM in ^{223}Rn that is expected to be 400–600 times greater than that in ^{199}Hg , which currently sets the best limits on several mechanisms of CP violation. With $|d(^{199}\text{Hg})| < 2.10 \times 10^{-28} e \cdot \text{cm}$ [12], a measurement of the ^{223}Rn EDM with a sensitivity of $10^{-26} e \cdot \text{cm}$ or better would be a significant improvement. This appears feasible at current and future rare isotope production facilities using NMR with laser-polarized noble gases [13] combined with γ -ray anisotropy [14] or β

asymmetry [15] detection techniques. Earlier work at ISOLDE [14] demonstrated polarization of ^{209}Rn and ^{223}Rn by spin exchange with laser optically pumped potassium and measured the magnetic moment of ^{209}Rn ; however, the polarization and relaxation mechanisms were not studied in detail and cell coatings were not explored. This article reports new techniques applied at the Stony Brook Francium Lab [16] to measure, for the first time, the temperature dependence of radon polarization in coated and uncoated glass cells at several temperatures.

The setup used to collect and transfer radon to an optical pumping cell is shown in Fig. 1. The cells were blown from boro-silicate glass (i.e., Pyrex) and attached to a hand-operated glass valve. Uncoated cells and cells coated with octadecyltrichlorosilane [13] were studied. Cell coatings have been used to reduce the sticking-time and wall relaxation of xenon isotopes [4], but enhanced relaxation due to electric quadrupole interactions within the coating have also been reported for the spin-3/2 isotope ^{131}Xe [17]. Sufficient quantities of neutron-rich ^{223}Rn could not be produced; however, ^{209}Rn ($\mathbf{I} = 5/2$, $T_{1/2} = 28.5$ min) and ^{223}Rn ($\mathbf{I} = 7/2$, $T_{1/2} = 23.2$ min) have similar magnetic dipole and electric quadrupole moments and are expected to have similar spin-exchange and cell-wall interactions. A 91 MeV beam of ^{16}O incident on a heated gold target generated ^{209}Fr ($T_{1/2} = 50.0$ s) by the reaction $^{197}\text{Au}(^{16}\text{O},4n)$. The ^{209}Fr released from the target was accelerated to 5 keV, electrostatically focused, and implanted in a zirconium foil where it decayed by electron capture to ^{209}Rn with a branching ratio of 11%. The francium was implanted for about two half-lives of ^{209}Rn (i.e., 40–60 min).

After implantation, the foil was heated to about 1000°C with the chamber isolated from the beamline and pumps. At this temperature, radon rapidly diffused out of the foil [18] and was frozen in the optical pumping cell, which was immersed in liquid nitrogen. Valve V2 was then closed and about one atmosphere of nitrogen was added to the cell to act as a buffer gas for optical pumping. The cell was then isolated from the rest of the vacuum system by shutting valve V4,

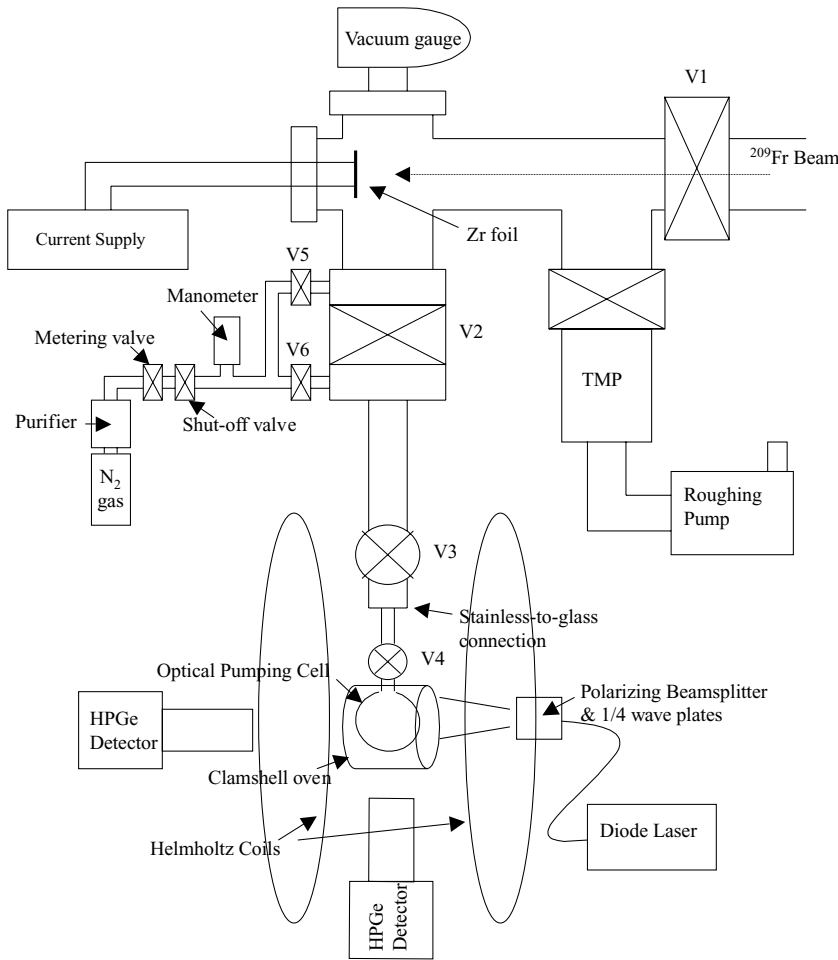


FIG. 1. A schematic diagram of the experimental apparatus used to transfer radon to the optical pumping cell.

and a two-piece glass oven was placed around it, allowing it to be heated to temperatures in the range 150 to 220°C. Up to about one million ^{209}Rn atoms were transferred to the cell in each cycle. The optical pumping cell was held in a uniform magnetic field of about 10.5 G and illuminated by circularly polarized laser light from a coherent fiber-coupled diode laser array (Coherent FAP System) tuned to the Rb-D1 line. Spin-exchange collisions [19] transferred the rubidium valence electron polarization to the ^{209}Rn nuclei. The resulting angular distribution of γ rays was monitored by two 100% (relative to NaI) Ortec HPGe detectors at 0° and 90°. The detectors were placed as close to the cell as possible, i.e., about 5 cm from the center of the cell. In an earlier run [20] a Eurisys Clover detector (four crystals, each with 25% internal efficiency, with their signals summed) was used at 0°. At each temperature laser-off data were used to determine the relative detector solid angles and efficiencies. γ -ray spectra before and after transfer are shown in Fig. 2.

The γ -ray angular distributions depend on the Zeeman levels populated by ^{209}Rn decay to excited states of ^{209}At , the spins of the states, and the multipolarity of the transitions [21]. Table I includes the multipole mixing ratios (δ) of the four prominent lines and the spin transitions involved. Following the convention of Ref. [22], $\delta^2 = a_1^2/a_2^2$, where $a_1 = 1$ for a pure dipole transition, $a_2 = 1$ for a pure quadrupole transition,

and $a_1^2 + a_2^2 = 1$. The anisotropy data as a function of temperature are shown in Figs. 3 and 4 for the 337 and 745 keV γ rays, respectively. The uncoated cell data up to 200°C combine data from the second run with data from an earlier run that were presented in the conference proceedings published as Ref. [20]. The anisotropy is given by the ratio

$$R = \frac{(n_{0^\circ}/n_{90^\circ})_{\text{LON}}}{(n_{0^\circ}/n_{90^\circ})_{\text{LOFF}}}, \quad (1)$$

where n_{0°/n_{90° is the background-corrected ratio of photo peak counts in the 0° detector to counts in the 90° detector calculated for data with the laser on (LON) and with the laser off (LOFF). Data for the 408 keV γ ray were consistent with no anisotropy, due in part to the cascade that accounts for about half of the

TABLE I. The four main ^{209}Rn γ ray lines [30] (from the *Table of Isotopes*) are listed together with the corresponding absolute intensity I_γ , spin transition, and multipole mixing ratio (δ).

E_γ (keV)	I_γ (%)	Spin transition	δ (Ref. [30])
337.45	14.5	$7/2 \rightarrow 7/2$	∞
408.32	50.3	$7/2 \rightarrow 9/2$	0
689.26	9.7	$7/2 \rightarrow 7/2$	>3.57
745.78	22.8	$7/2 \rightarrow 9/2$	>2.86

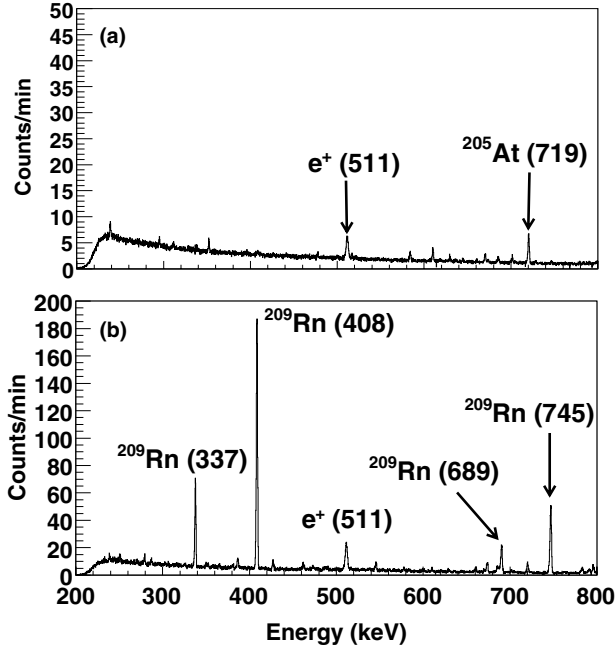


FIG. 2. γ -ray spectra from the 0° detector. Spectrum (a) was taken over about an hour during the implantation of the ^{209}Fr beam in the Zr foil and spectrum (b) was taken over the first 10 min after transfer of the ^{209}Rn to the optical pumping cell. Note the different vertical scales. The ^{205}At results from ^{209}Fr α decay.

population of the 408 keV level in ^{209}At . The 689 keV line could not be reliably extracted from the background.

The measured anisotropies depend on the alignment, i.e., the second moment of the nuclear sublevel population distribution. The alignment results from the combination of spin-exchange from the polarized rubidium, a magnetic

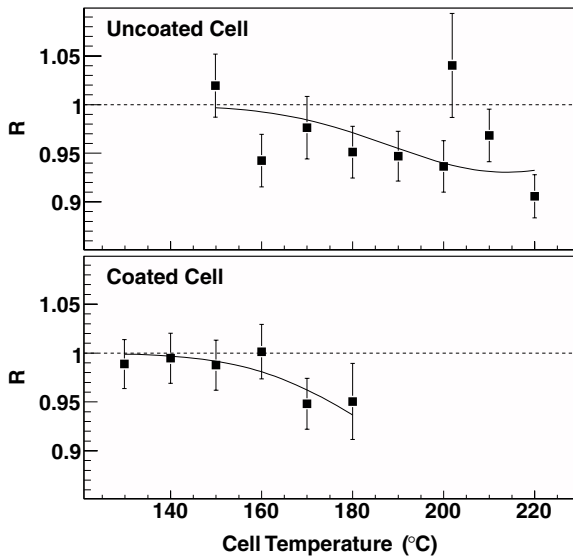


FIG. 3. Anisotropy data from the coated and uncoated cells for the 337 keV ^{209}Rn γ ray. For the uncoated cell, data from the two runs are displayed. R is the ratio defined in Eq. (1), and the solid curves are fits to the temperature dependence using $\sigma_{\text{SE}} = 2.5 \times 10^{-5} \text{ \AA}$.

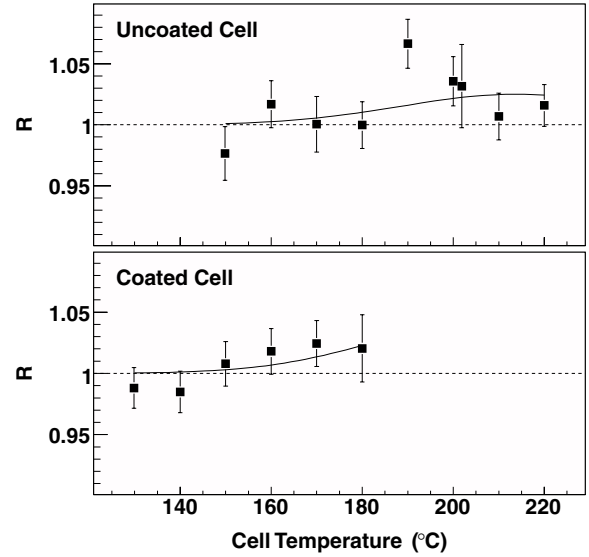


FIG. 4. Anisotropy data for the 745 keV ^{209}Rn γ ray displayed in the same manner as the 337 keV data in Fig. 3. The fits use $\sigma_{\text{SE}} = 2.5 \times 10^{-5} \text{ \AA}$ and $\delta = \infty$.

dipole interaction, and relaxation, which is dominated by electric quadrupole interactions. (Quadrupole relaxation (Γ_2) has been shown to be much stronger than dipole relaxation (Γ_1) in ^{131}Xe [17] and ^{21}Ne [23].) At low temperatures, the rubidium is almost completely polarized as optical pumping overcomes all spin destruction processes, but the radon wall sticking time is greater. At higher temperatures the rubidium polarization slowly drops as the laser light is absorbed to balance increased spin destruction, but the wall interaction decreases exponentially, i.e., with an expected Arrhenius-type temperature dependence [24],

$$\Gamma_2(T) = \Gamma_2^\infty e^{T_0/T}, \quad (2)$$

where $k_B T_0$ is the binding energy of the radon to the cell wall. The anisotropy data in Figs. 3 and 4 show that the alignment of ^{209}Rn in the coated cell becomes significant at a temperature lower than that for the uncoated cell. This indicates that $\Gamma_2(T)$ is less in the coated cell, apparently in disagreement with the observation in ^{131}Xe reported in Ref. [17].

For a nuclear spin I , there are $2I + 1$ coupled rate equations that govern the steady state moments of the polarization [23,25], and the radon polarization moments result from the interplay of processes that can be parametrized by the rubidium polarization P_{Rb} , the rubidium-radon spin-exchange rate γ_{SE} , and the radon quadrupole relaxation rate Γ_2 . The averaged rubidium polarization was directly measured using the change in fluorescence of the Zeeman sublevels when quenched by electron spin resonance [26]. Thus the unknown parameters are γ_{SE} and $\Gamma_2(T)$. The spin-exchange rate is

$$\gamma_{\text{SE}} = [\text{Rb}] \langle \sigma_{\text{SE}} v \rangle, \quad (3)$$

in which the temperature dependence enters through the velocity-averaged rate constant $\langle \sigma_{\text{SE}} v \rangle$ and rubidium number

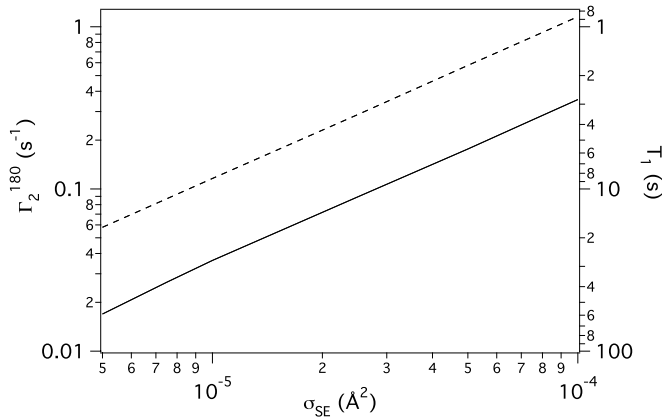


FIG. 5. Relaxation rates, Γ_2 , obtained from best fits to the 337 keV data for the two cells as a function of σ_{SE} . The axis on the right shows the cell relaxation time used to estimate the EDM sensitivity. The solid line is for the coated cell and the dashed line is for the uncoated cell.

density [Rb], with temperature dependence given by $[Rb] = 10^{9.318 - \frac{4040}{T}} / k_B T$ [27].

The 337 keV γ -ray anisotropy data were fit to a model based on radon polarization and the spin sequences of the γ -ray decays for each cell temperature [28]. Because σ_{SE} and T_0 are varied, the best fit value for Γ_2^∞ was determined. The quadrupole relaxation rate $\Gamma_2(T)$ given by Eq. (2) does not depend strongly on T_0 ; i.e., the measured anisotropies constrain the total relaxation rate but do not effectively separate Γ_2^∞ from the binding energy $k_B T_0$. The data and analysis are summarized in Fig. 5, where $\Gamma_2(T = 180^\circ)$ derived from the fits is plotted as a function of σ_{SE} for the coated cell and the uncoated cell. Varying T_0 over the range 100 to 600 K has a negligible effect on this result. These data do not effectively constrain σ_{SE} ; however, Walker has calculated the cross sections for alkali-metal-noble-gas spin exchange,

providing impressive agreement with measurements for a large number of cases [29]. Walker's result for Rb- ^{209}Rn is $\sigma_{SE} = 2.5 \times 10^{-5} \text{ \AA}^2$, which was used to produce the solid curves in Figs. 3 and 4.

In summary, radon has been collected and polarized by spin exchange with laser polarized rubidium in coated and uncoated glass cells. The temperature dependence of anisotropies has been measured and used to parametrize polarization and relaxation rates for ^{209}Rn , which are expected to be similar for ^{223}Rn . These results are significant for the radon EDM measurement under development at TRIUMF. The ISAC facility is expected to produce ^{223}Rn at a rate of $10^7/\text{s}$, more than 1000 times the rates for this work, and approximately 500 million radon atoms can be collected in a measurement cell. The uncertainty of the EDM measured using the anisotropy signal is

$$\delta_d = \frac{\hbar}{2ET_2} \sqrt{\frac{1}{A^2(1-B)^2N}}, \quad (4)$$

where E is the magnitude of the electric field, T_2 is the coherence time of the polarization, A is the analyzing power of the measurement (i.e., the change in the signal due to a change in polarization), N is the total number of γ -ray photons detected, and B is the fraction of those photons due to background. Using $T_2 = 15$ s, based on Fig. 5 for $\sigma_{SE} = 2.5 \times 10^{-5} \text{ \AA}^2$, $A = 0.1$, $B = 0.01$, and $E = 10$ kV/cm [13], a sensitivity of better than $10^{-26} e \cdot \text{cm}$ is possible with $N = 10^{12} \gamma$'s. Assuming a 400-fold enhancement for ^{223}Rn , this would improve sensitivity to sources of CP violation by an order of magnitude or more compared to the limits set by the ^{199}Hg measurements.

This work was supported by the U. S. National Science Foundation, the Department of Energy, and the Natural Sciences and Engineering Research Council of Canada.

- [1] H. Kauczor, R. Surkau, and T. Roberts, *Eur. Radiol.* **8**, 820 (1998).
- [2] T. E. Chupp, R. J. Holt, and R. G. Milner, *Annu. Rev. Nucl. Part. Sci.* **72**, 373 (1994).
- [3] K. P. Coulter *et al.*, *Nucl. Instrum. Methods Phys. Res. A* **288**, 463 (1990).
- [4] X. Zeng *et al.*, *Phys. Rev. A* **31**, 260 (1985).
- [5] S. D. Swanson *et al.*, *Magn. Reson. Med.* **38**, 695 (1997).
- [6] T. E. Chupp *et al.*, *Phys. Rev. Lett.* **63**, 1541 (1989).
- [7] F. Cane, D. Bear, D. F. Phillips, M. S. Rosen, C. L. Smallwood, R. E. Stoner, R. L. Walsworth, and V. A. Kostelecky, *Phys. Rev. Lett.* **93**, 230801 (2004).
- [8] A. G. Cohen, D. B. Kaplan, and A. E. Nelson, *Annu. Rev. Nucl. Part. Sci.* **43**, 27 (1993).
- [9] W. C. Haxton and E. M. Henley, *Phys. Rev. Lett.* **51**, 1937 (1983).
- [10] V. Spevak, N. Auerbach, and V. V. Flambaum, *Phys. Rev. C* **56**, 1357 (1997).
- [11] J. Engel, J. L. Friar, and A. C. Hayes, *Phys. Rev. C* **61**, 035502 (2000).
- [12] M. V. Romalis, W. C. Griffith, J. P. Jacobs, and E. N. Fortson, *Phys. Rev. Lett.* **86**, 2505 (2001).
- [13] M. A. Rosenberry and T. E. Chupp, *Phys. Rev. Lett.* **86**, 22 (2001).
- [14] M. Kitano *et al.*, *Phys. Rev. Lett.* **60**, 2133 (1988).
- [15] E. D. Commins and P. H. Bucksbaum, *Weak Interactions of Quarks and Leptons*, (Cambridge University Press, Cambridge, UK, 1983).
- [16] J. E. Simsarian *et al.*, *Phys. Rev. Lett.* **76**, 3522 (1996).
- [17] Z. Wu, W. Happer, M. Kitano, and J. Daniels, *Phys. Rev. A* **42**, 2774 (1990).
- [18] T. Warner *et al.*, *Nucl. Instrum. Methods Phys. Res. A* **538**, 135 (2005).
- [19] T. G. Walker and W. Happer, *Rev. Mod. Phys.* **69**, 629 (1997).
- [20] E. R. Tardiff *et al.*, *Nucl. Instrum. Methods Phys. Res. A* **579**, 472 (2007).
- [21] H. A. Tolhoek and J. A. M. Cox, *Physica* **19**, 101 (1953).
- [22] C. D. Hartogh, H. A. Tolhoek, and S. R. de Groot, *Physica* **20**, 1310 (1954).
- [23] T. E. Chupp and R. J. Hoare, *Phys. Rev. Lett.* **64**, 2261 (1990).
- [24] W. Happer, *Rev. Mod. Phys.* **44**, 169 (1972).

- [25] T. E. Chupp and K. P. Coulter, Phys. Rev. Lett. **55**, 1074 (1985).
- [26] E. Babcock, I. A. Nelson, S. Kadlecěk, and T. G. Walker, Phys. Rev. A **71**, 013414 (2005).
- [27] T. J. Killian, Phys. Rev. **27**, 578 (1926).
- [28] E. R. Tardiff *et al.* (in preparation).
- [29] T. G. Walker, Phys. Rev. A **40**, 4959 (1989).
- [30] *Table of Isotopes*, 8th ed., edited by V. S. Shirley (Wiley & Sons, New York, 1996), Vol. II, pp. 2598–2600.